

**DEVELOPMENT OF A HIGH-SPEED ON-OFF VALVE  
FOR SWITCH-MODE CONTROL OF HYDRAULIC CIRCUITS  
WITH FOUR-QUADRANT CONTROL**

**Jeslin J. Wu**

Mechanical Energy & Power Systems Lab  
Worcester Polytechnic Institute  
Worcester, Massachusetts 01609

**James D. Van de Ven**

Mechanical Energy & Power Systems Lab  
Worcester Polytechnic Institute  
Worcester, Massachusetts 01609

**ABSTRACT**

Hydraulic circuits are typically controlled by throttling valves or variable displacement pump/motors. The first method throttles fluid for a desired pressure output and excess energy is lost through heat. While variable displacement pumps are more efficient, they are often large and expensive. An alternate method is the switch-mode control of hydraulic circuits through high-speed on-off valves. The proposed on-off valve design makes use of a continuously rotating disc to modulate flow between on and off states; the average power output or pulse duration is determined by the relative phase shift between the input and output ports. The addition of a directional valve to the high-speed three-way valve allows any fixed displacement actuator to behave like a virtually variable displacement unit that is capable of four-quadrant control. In this paper a mathematical model focusing on the throttling, compressibility, internal leakage and viscous friction losses is developed and utilized to optimize the valve design for highest efficiency.

**INTRODUCTION**

An emerging technology to decrease our dependence on fossil fuels and combat pollution is hydraulic hybrid vehicle power trains [1]. When the vehicle brakes, its kinetic energy is used to power a reversible pump/motor, which pumps low-pressure hydraulic fluid from a reservoir into the high-pressure accumulator. During acceleration, the pump/motor is reversed and the pressurized fluid is used to drive the vehicle. In the hydraulic hybrid drive train, the pump/motor must operate in all four-quadrants, defined as the ability to apply both positive and negative torque, and be able to operate in the forward and reverse directions.

Hydraulic machineries are typically controlled by two different methods: throttling valves and variable displacement pumps. Throttling valves provide fast response by throttling the fluid to the desired output pressure while excess power is converted to waste heat. Variable displacement pumps are more efficient; however, they are large and expensive [2].

An emerging method of hydraulic system control is switch-mode control through high-speed on-off valves, illustrated in Figure 1. The valve rapidly and continuously switches between efficient on and off states in a pulse-width modulation manner. The average pressure at the hydraulic pump/motor is controlled by modulating the duty cycle, defined as the time in the on position divided by the switching time. This essentially allows any fixed displacement pump/motor to behave like a virtually variable displacement unit. The check valves shown in the circuit permit flow to and from the pump/motor when the on-off valve is blocked during switching events.

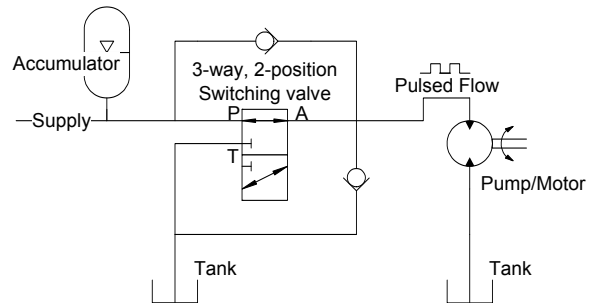


**Figure 1. Hydraulic circuit of a high-speed on-off valve**

The high-speed on-off valve described above, however, does not allow a reversal of torque at the hydraulic pump/motor, as required for regeneration capabilities. To resolve this issue, a four-way, three-position directional valve can be integrated into

the hydraulic circuit as shown in Figure 2. The directional valve allows the output of the high-speed valve to be directed to either port of a pump/motor, while the other port is connected to tank. This allows torque reversal of the pump/motor. Because the flow through the valve is bi-directional, generation and regeneration is possible in both forward and reverse direction, hence four quadrant control.

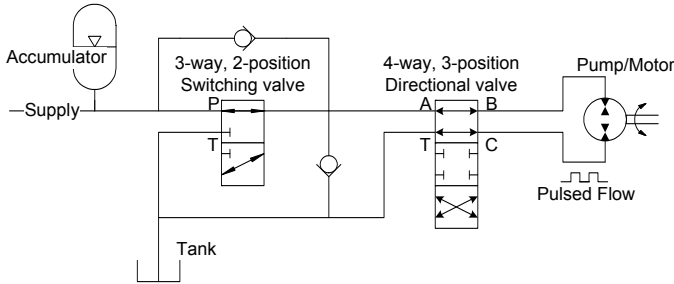


**Figure 2. Hydraulic circuit of a high-speed on-off valve with regeneration capabilities**

This paper presents a novel design of a disc-style high-speed on-off valve for switch-mode control of hydraulic circuits with four-quadrant control. A first generation prototype of the switching valve circuit shown in Figure 1 has been developed and tested [3]. This first generation valve demonstrated the disc-style phase-shift design, which makes use of a continuously rotating disc to modulate flow between efficient on and off states. The average pulse duration is determined by the relative phase shift between the input and output ports of the switching valve. The second generation prototype, discussed in this paper, incorporates a directional valve to allow for four-quadrant control of a hydraulic actuator. The directional valve is achieved through making dual use of the phase shift of the output port. A mathematical model focused on the throttling, compressibility, internal leakage, and viscous friction losses is developed and presented, followed by an optimization of the valve geometry for highest efficiency.

### FIRST GENERATION PROTOTYPE

As mentioned, a first generation prototype valve designed for an operating pressure 6.9 MPa, a flow rate of  $1.26 \times 10^{-4}$  m/s, and a switching frequency of 100 Hz made use of a continuously rotating disc to modulate flow between on and off states [3]. The relative phase shift between the input and output ports determines the pulse duration.

The phase shift concept is depicted in Figure 3. Subplot (a) shows high-pressure fluid directed from Port P through Section 1A of Tier 1 to Section 2 of Tier 2 and finally out through Port A. Recognizing that all of the valve discs rotate at the same angular velocity, after a  $\pi/2$  rotation of the discs, as shown in subplot (b), the pathway previously mentioned is blocked and the flow is directed from Port T (low-pressure fluid) through Section 1B of Tier 1 to Section 2 of Tier 2 and out through A.

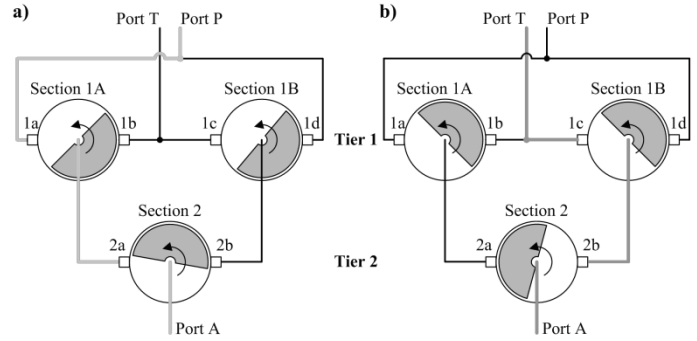


**Figure 3. Phase shift concept showing two different flow paths**

The flow diversion as a result of the phase shift is shown in Figure 4 below. The shaded sections denote flow from Section 1 to 2. Sections 1A and 1B remain in sync with each other, while Section 2 varies from 0 to  $\pi$  phase with respect to Section 1. This effectively creates a continuously variable duty ratio from 0 to 1.

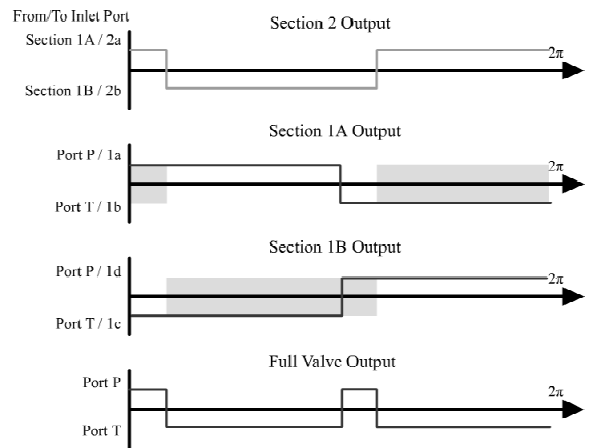


**Figure 4. Flow diversion as a result of the phase shift. Shaded regions denote flow from Section 1 to 2. Labeling is consistent with Figure 3 above.**

A disc-style architecture of the on-off valve can be created through a kinematic inversion of the schematic in Figure 3 and by redirecting the flow to move axially, as illustrated in Figure 5. In this setup, three discs – Tier 1, the valve plate, and Tier 2 – are stacked on top of each other. The two sub-valves of Section 1 are combined into a single tier, Tier 1. The duty ratio is modulated by varying the phase of Tier 2 relative to the fixed Tier 1. A new continuously rotating disc, the valve plate, is introduced to generate the switching cycles. Note that the ports in Tier 1 and Tier 2 (P, T, and A) are replicated to provide pressure balancing.

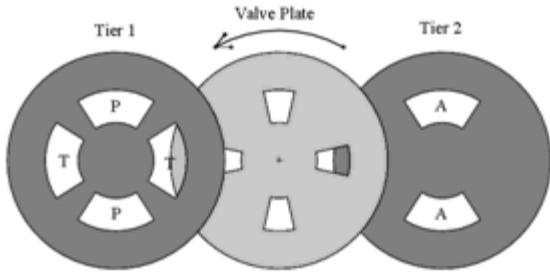


**Figure 5. Kinematic inversion of Figure 3. Section 1 sub-valves have been combined into Tier 1. Tier 2 changes phase relative to the fixed Tier 1. The valve plate generates the pulses.**

**SECOND GENERATION PROTOTYPE**

The second generation valve aims to advance the previous design by enabling four-quadrant control of a hydraulic circuit, i.e. regeneration capabilities, improved packaging, higher actual switching frequency, improved phase-shift control accuracy, and higher efficiency. The valve design targets are an operating pressure of 20.7 MPa, a flow rate of  $1.26 \times 10^{-4} \text{ m}^3/\text{s}$ , and a switching frequency of 100 Hz. Check valves will also be integrated into the valve to prevent cavitations and pressure spikes.

The on-off valve with the integrated directional valve is illustrated in Figure 6. A cross port is incorporated into Tier 2 for the tank inlet into the four-way, three-position valve. The output ports of the on-off valve are combined to a single port in Tier 2, which serves as the Port A input into the directional valve. An additional tier, Tier 3, is introduced to incorporate the two output ports – Port B and Port C. The relative phase shift between Tier 2 and Tier 3 will direct the flow from Port A to either port of a pump/motor and connect the other port to tank.

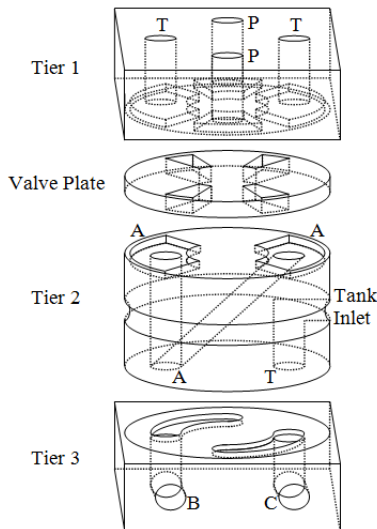


**Figure 6. Integrated directional valve into the high-speed on-off valve**

**Numerical Model**

A numerical model focused on compressibility, throttling, viscous friction, and internal leakage energy losses of the high-speed will now be presented.

Figure 7 illustrates the key geometry features of the on-off valve. The figure shows one replication of ports on the valve, defined by  $N$ . The number of replications determine the number of on or off cycles in a full revolution of the valve plate. The inner and outer radius of the valve ports are defined as  $R_i$  and  $R_o$ , respectively. The ports on the valve plate and the output ports of Tier 2 span an angle of  $\delta$ ; the ports of Tier 1 and the input ports of Tier 2 span an angle of  $\gamma$ ; and the ports of Tier 3 span an angle of  $\pi/2 - \delta$ . Since  $\delta + \gamma = \pi/N$ , the valve will be completely blocked twice each switching cycle.

The angular position of the valve plate,  $\theta$ , is defined as zero degrees when the valve plate ports are completely blocked by the Tier 1 ports. The phase angle,  $\alpha$ , is defined as zero degrees when Port A of Tier 2 is aligned with Port T of Tier 1 and  $\pi/N$  when it aligns with Port P.  $A_1$  is the variable orifice created by the overlap of Tier 1 with the valve plate,  $A_2$  is the variable orifice created by the overlap of the input into Tier 2 with the valve plate, and  $A_3$  is the area created between the output of Tier 2 with Tier 3.

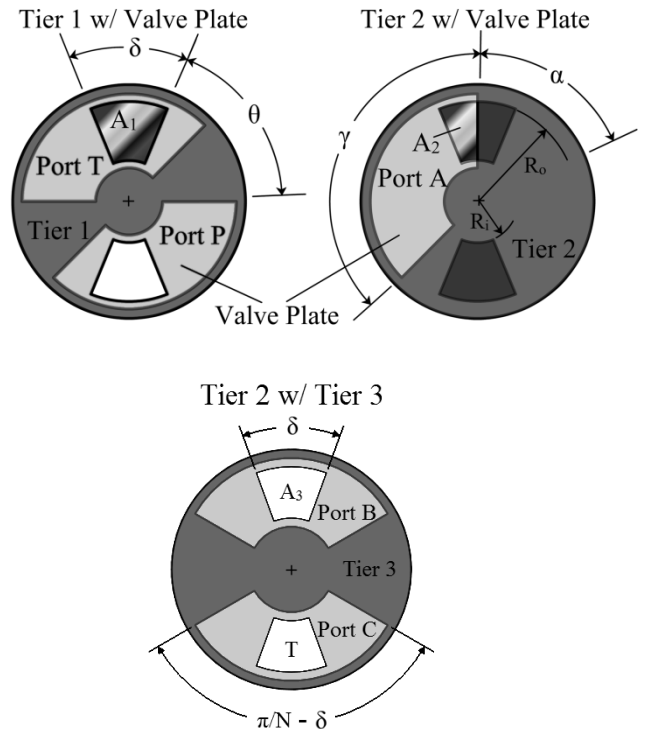


**Figure 7. Key geometry features of the on-off valve. The rotation of the valve plate,  $\theta$ , is defined as zero degrees when the valve plate ports are fully blocked and about to transition to Port T. The phase angle,  $\alpha$ , is defined as zero degrees when Port A of Tier 2 lines up with Port T and  $\pi/2$  when it lines up with Port P.**

### Compressibility Losses

A major form of energy loss is a result of the compression of the fluid due to fluctuating pressures. The volume of fluid experiencing pressure fluctuations, labeled the switched volume, includes a portion of the internal area of the valve and fluid conductors to the hydraulic pump/motor. This energy loss can be calculated using the following equation:

$$E_{comp} = (P_{high} - P_{tank}) \Delta V \quad (1)$$

where  $P_{high}$  is the supply pressure,  $P_{tank}$  is the tank pressure and  $\Delta V$  is the change in volume of the fluid due to the fluctuating pressures.

By definition of the bulk modulus, which is the pressure increase necessary to cause a relative decrease in volume, the change in volume can be calculated using the following equation:

$$\Delta V = \frac{(P_{high} - P_{tank}) V_{switch}}{\beta_e} \quad (2)$$

where  $V_{switch}$  is the internal volume of the fluid and  $\beta_e$  is the effective bulk modulus.

The bulk modulus depends on the air content, the pressure and the temperature of the fluid, and the elasticity of the wall; it therefore is complicated to calculate. For this reason, a simplified equation proposed by Merritt [4] is used to calculate the effective bulk modulus:

$$\frac{1}{\beta_e} = \frac{1-R}{\beta_{oil}} + \frac{R}{P_{high} k} \quad (3)$$

where  $\beta_{oil}$  is the bulk modulus of air-free oil,  $R$  is the volumetric fraction of air in the oil at atmospheric pressure, and  $k$  is the specific heat of air.

### Viscous Friction Losses

A second form of energy loss is a result of the shearing of fluid due to the rotating valve plate. The two main regions of viscous friction losses are the following:

1. Circumferential: between the outer diameter of the valve plate and the cylindrical bore
2. Plate: between the faces of the valve plate and the neighboring Tier

Petroff's equation [5] gives the method of calculating the torque on the circumference of the valve plate:

$$T_{journal} = \frac{2\pi\omega\mu tr^3}{c_b} \quad (4)$$

where  $\omega$  is the angular velocity of the valve plate,  $\mu$  is the absolute viscosity of the fluid,  $t$  is the thickness and  $r$  is the outer radius of the valve plate, and  $c_b$  is the radial clearance between the valve plate and the bore.

For the forces between the faces of the rotating valve plate and the stationary tiers, Newton's postulate calculates that the frictional torque on the switching area as:

$$\begin{aligned} T_{plate} &= Fr = \frac{\mu Au}{c_f} r \\ &= \int_0^{2\pi} \int_{r=R_i}^{r=R_o} \mu \frac{(r \cdot dr \cdot d\theta)(\omega r)}{c_f} r \\ &= \frac{\pi\omega\mu}{2c_f} (R_o^4 - R_i^4) \end{aligned} \quad (5)$$

where  $A$  is the area of the valve plate,  $c_f$  is the film plate thickness, and  $R_o$  and  $R_i$  are the outer and inner radius of the area of interest, respectively. The above equation is applied to both the front and back face of the valve plate. Note that since the area included in the above equation includes the openings of the valve plate and the tiers, the predicted torque should be higher than the actual.

The energy loss due to viscous friction is therefore:

$$E_{f,loss} = \omega(T_{journal} + T_{plate,front} + T_{plate,back}) \quad (6)$$

### Throttling Losses

Another form of energy loss is through the throttling of the fluid as the valve transitions between the on and off states. During each revolution, there are  $2N$ , or in this case four, on-off cycles, where  $N$  is the number of on or off cycles per revolution. Two switches occur every cycle, resulting in  $4N$ , or eight, switches per revolution. The duration between each switch is determined by the duty ratio, which is controlled by the relative phase angle of the Tier 1 and Tier 2 ports.

To calculate the throttling losses, the open areas of each port in the valve must first be determined. Between Tier 1 and the valve plate, the area is described by:

$$A_1(\theta) = \begin{cases} \frac{N\theta}{2} (R_o^2 - R_i^2) & \text{for } 0 \leq \theta \bmod \frac{\pi}{N} < \delta \\ \frac{N\delta}{2} (R_o^2 - R_i^2) & \text{for } \delta \leq \theta \bmod \frac{\pi}{N} < \gamma \\ \frac{\pi - N\theta}{2} (R_o^2 - R_i^2) & \text{for } \gamma \leq \theta \bmod \frac{\pi}{N} < \frac{\pi}{N} \end{cases} \quad (7)$$

where  $\theta$  modulo  $\pi/N$  maintains the evaluated angle between 0 and  $\pi/N$  for multiple rotations.

The area between the valve plate and Tier 2 is described by:

$$\begin{aligned} A_2(\theta) &= \begin{cases} \frac{N(\theta - \alpha)}{2} (R_o^2 - R_i^2) & \text{for } 0 \leq \theta - \alpha \bmod \frac{\pi}{N} < \delta \\ \frac{N\delta}{2} (R_o^2 - R_i^2) & \text{for } \delta \leq \theta - \alpha \bmod \frac{\pi}{N} < \gamma \\ \frac{\pi - N(\theta - \alpha)}{2} (R_o^2 - R_i^2) & \text{for } \gamma \leq \theta - \alpha \bmod \frac{\pi}{N} < \frac{\pi}{N} \end{cases} \end{aligned} \quad (8)$$

Finally, the open area between Tier 2 and Tier 3 is described by:

$$A_3 = \begin{cases} \frac{\delta}{2} (R_o^2 - R_i^2) & \text{for } -\delta \leq \alpha \bmod \pi < \frac{\pi}{2} + \delta \\ 0 & \text{for } \frac{\pi}{2} + \delta \leq \alpha \bmod \pi < \pi \end{cases} \quad (9)$$

The open areas of each port in the valve for 0.25 duty ratio is illustrated in Figure 8 below. The values used to generate the plot are given in Table 1 and Table 2. Note that the open area between Tier 2 and Tier 3,  $A_3$ , is a function of the duty ratio only and does not vary with the angular position of the valve plate.

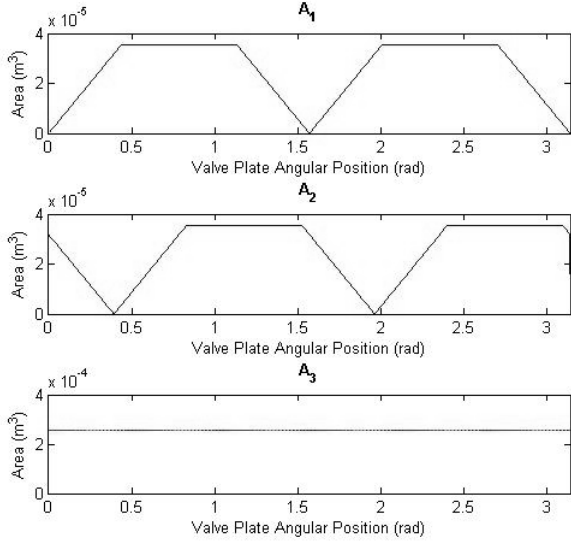


**Figure 8. Open areas for Tier 1 (top), Tier 2 (middle) and Tier 3 (bottom) as a function of angle of rotation of valve plate (shown for 0.25 duty ratio).**

Assuming the open areas of the two restrictions in the three-way, two-position, valve can be modeled as orifices in series [6], the full flow pressure drop across valve is calculated as follows:

$$\begin{aligned} \Delta P &= \Delta P_{Tier1} + \Delta P_{Tier2} \\ &= \frac{\rho}{2} \left( \frac{Q}{C_d A_1} \right)^2 + \frac{\rho}{2} \left( \frac{Q}{C_d A_2} \right)^2 \\ &= \frac{\rho Q^2 (A_1^2 + A_2^2)}{2 C_d^2 A_1^2 A_2^2} \end{aligned} \quad (10)$$

where  $\rho$  is the density of the fluid,  $Q$  is the flow rate into the three-way, two-position valve and  $C_d$  is the discharge coefficient.

The pressure drop across the switching valve for 0.25 duty ratio is shown in Figure 9 below. The values used to generate the plot are given in Table 1 and Table 2. Note that there are four pressure spikes in the plot corresponding to the four on-off switches per revolution of the valve plate.

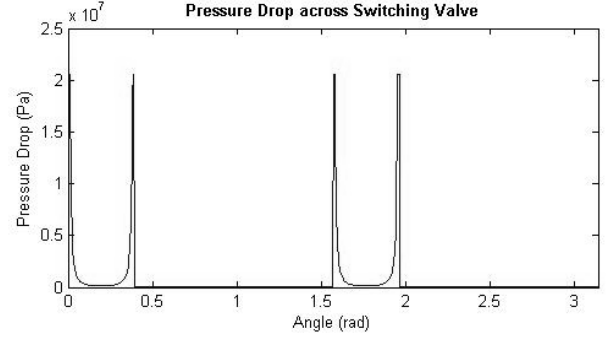


**Figure 9. Plot of pressure drop across the switching valve for 0.25 duty ratio**

To prevent cavitations during motoring and pressure spikes during pumping, check valves are integrated into the valve. The following equations are used to incorporate the effects of check valves on the pressure drop in the valve:

During motoring, the low-pressure check valve opens if  $\Delta P > P_s - P_{tank} + \Delta P_{check}$  and the pressure drop across the valve is:

$$\Delta P = P_s - P_{tank} + \Delta P_{check} \quad (11)$$

where  $P_s$  is the supply pressure – either  $P_{high}$  or  $P_{tank}$  and  $\Delta P_{check}$  is the crackling pressure of the check valve.

During pumping, the high-pressure check valve opens if  $\Delta P > P_{high} - P_s + \Delta P_{check}$  and the pressure drop across the valve is:

$$\Delta P = P_{high} - P_s + \Delta P_{check} \quad (12)$$

The flow through the three-way, two-position valve is therefore:

$$Q_{valve} = C_d A_1 A_2 \sqrt{\frac{2 \Delta P_1}{\rho (A_1^2 + A_2^2)}} \quad (13)$$

and the flow through the check valve is:

$$Q_{check} = Q - Q_{valve} \quad (14)$$

The pressure drop across the four-way, three-position valve is assumed to be negligible as the directional valve can simply be modeled as a fixed orifice.

The total power loss can therefore be expressed as:

$$P_{throttling} = \Delta P Q_{valve} + \Delta P_{check} Q_{check} \quad (15)$$

### Internal Leakage Losses

The final primary form of energy loss is the internal leakage of the valve. There are two primary paths of leakage:

1. Radially outwards to the bore, which is held at tank pressure
2. Circumferentially to the tank pressure ports

These leakages take place in two main areas:

- Case A: Between Tier 1 and the front face of valve plate
- Case B: Between Tier 2 and the back face of the valve plate

The leakage between Tiers 2 and 3 is negligible as o-ring seals will be used between the faces.

The radial leakage can be calculated assuming parallel plate flow:

$$Q_{leak,rad} = \frac{Per \cdot c^3 \Delta P}{12\mu L} \quad (16)$$

where  $c$  is the clearance between the faces,  $\Delta P$  is the pressure differential, given by  $(P_{high} - P_{tank})$ ,  $L$  is the length of the leakage path, given by  $(R_b - R_o)$  and  $Per$  is the perimeter of the leakage path, given by the average arc length:

$$Per = \begin{cases} N\gamma \frac{R_b + R_o}{2} & \text{for Case A} \\ \frac{N}{2}(\gamma \cdot Duty + \delta(1 - Duty)) \frac{R_b + R_o}{2} & \text{for Case B} \end{cases} \quad (17)$$

where  $Duty$  is the duty ratio, given by  $\alpha N/\pi$ .

The power loss due to the radial leakage is therefore:

$$P_{leak,rad} = Q_{leak,rad} \Delta P \quad (18)$$

The circumferential leakage is complicated by the rotating valve plate, which creates the following variable leakage lengths:

1. When the ports are opening:
  - a) Orifice flow is first assumed
  - b) As the length of the leakage path,  $L$ , increases, variable length parallel plate flow is assumed
2. When the ports are fully opened:
  - a) Constant length parallel plate flow is assumed

This process is reversed when the ports are closing.

To determine the angle at which the flow will transition from orifice to parallel plate flow, the orifice equation is equated to the parallel plate equation:

$$Q_{orifice} = Q_{plate} \\ C_d A \sqrt{\frac{2}{\rho} \Delta P} = \frac{bc^3 \Delta P}{12\mu L} \quad (19)$$

where  $b$  is the width and  $c$  is the distance between the plates. The area,  $A$ , is given by  $2bc$  and the flow length,  $L$ , by  $\theta(R_i - R_o)/2$ . The flow transition angle is therefore:

$$\theta_{trans} = \frac{c^2}{6\mu C_d (R_i - R_o)} \sqrt{\frac{\rho \Delta P}{2}} \quad (20)$$

Recognizing that the leakage cycle takes place  $2N$  times per revolution of the valve plate, and there are  $2N$  leakage paths, the volume of leakage flow per revolution is:

$$V_{cir} = 4N^2 \int_{t=0}^{t=\frac{\pi}{N\omega}} Q(\theta) dt \quad (21)$$

defining  $\omega = d\theta/dt$ ,

$$V_{cir} = \frac{4N^2}{\omega} \int_{\theta=0}^{\theta=\frac{\pi}{N}} Q(\theta) d\theta \quad (22)$$

The energy loss from circumferential leakage is:

$$E_{leak,cir} = V_{circum} \Delta P \quad (23)$$

### Optimization

A MATLAB optimization code to determine the efficiencies of the valve with a given set of parameters was created. The code makes use of the function *fmincon* to find the values of the parameters that will minimize the energy losses and maximize the efficiency of the valve.

The geometry of the valve was optimized for the following parameters:  $R_i$ ,  $R_o$ ,  $\delta$ ,  $t$ ,  $R_b$ ,  $c_f$  and  $c_b$ . The model parameters can be found in Table 2 and the optimized variables are presented in Table 2.

**Table 1. Model parameters**

| Parameters                        | Values                                     |
|-----------------------------------|--|
| $N$                               | 2  |
| Duty                              | 0.25                                       |
| $f_{switch}$                      | 100 Hz                                     |
| $\omega$                          | 1500 rpm                                   |
| $V_{switch}$                      | $1.0 \times 10^{-3} \text{ m}^3$           |
| $P_{high}$                        | 20.7 MPa                                   |
| $P_{tank}$ (atmospheric pressure) | 101 kPa                                    |
| $Q$                               | $1.26 \times 10^{-4} \text{ m}^3/\text{s}$ |
| $\rho$ (Mobil DTE 25)             | 850 kg/m <sup>3</sup>                      |
| $\mu$                             | 0.0875 Pa-s                                |
| $\beta_{oil}$                     | 1.8 GPa                                    |
| $R$                               | 2 %  |
| $t$                               | 5 mm                                       |
| $C_d$                             | 0.61                                       |

**Table 2. Optimized parameters and values for second generation valve**

| Parameters                                       | Values   |
|--|----------|
| $R_i$  | 6.75 mm  |
| $R_o$  | 11.25 mm |
| $\delta$   | 25 °     |
| $t$  | 5 mm     |
| $R_b$  | 17.5 mm  |
| $c_f$ (Clearance between valve plate and Tier 1) | 12.7 μm  |
| $c_b$ (Clearance between valve plate and Tier 2) | 12.7 μm  |

### Efficiency and Losses

With the above optimized values, the efficiency of the valve was found to be approximately 50 % efficient at 0.25 duty ratio and 85 % efficient at 1 duty ratio as seen in Figure 10.

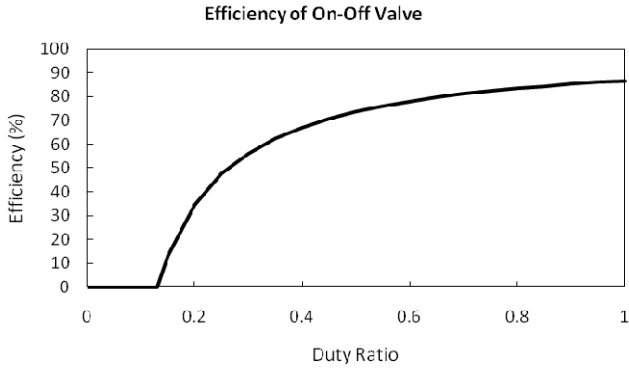


**Figure 10.** Plot of the variation of the efficiency with the change in duty ratio for the second generation valve

The contributions of each energy loss term to the total energy loss are presented in Table 3. The total energy loss is dominated by the compression of the fluid due to pressure fluctuations and the viscous friction due to shearing of the fluid.

**Table 3. Energy loss summary**

| Type             | Energy Loss (J) | Percentage Losses (%) |
|------------------|-----------------|-----------------------|
| Compressibility  | 5.27            | 33.0                  |
| Viscous Friction | 4.76            | 29.8                  |
| Leakage          | 3.65            | 22.8                  |
| Throttling       | 2.32            | 14.5                  |

## Prototype Design

Using the optimized geometry, a second generation prototype was designed, as seen in Figure 11.

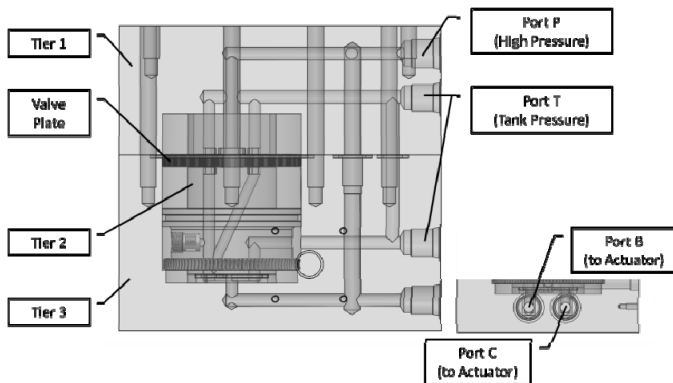


**Figure 11.** Main components and flow pathways of the second generation valve prototype

A phase shift between the fixed ports of Tier 1 and the input ports of Tier 2 determines the duty ratio of the on-off valve. The four-way, three-position directional valve is produced by the phase shift between the output of Tier 2 and output of the

on-off valve, Tier 3. A second inlet from tank is created on the circumference of Tier 2.

The phase angle of Tier 2 is modulated with a worm and wheel driven by a servo-motor. The angle of rotation of the servo-motor shaft with the worm, is controlled through an electrical pulse-width modulated signal. The built-in potentiometer allows for feedback on the angle of rotation.

The continuous rotation of the valve plate is provided by a DC motor mounted on the top of the Tier 1 section. The motor and the valve plate are connected through a shaft.

Check valves will be integrated into the valve to prevent cavitations while motoring and prevent pressure spikes while pumping. To minimize the response time of the check valve, the mass of the moving component must be minimized. To meet this need, a custom check valve was designed, which uses of a disc instead of a ball. Figure 12 depicts the custom check valve in the closed and open positions.

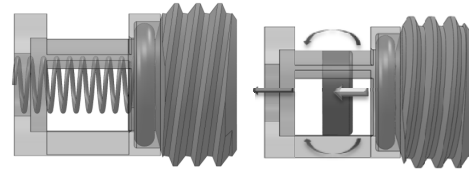


**Figure 12.** Custom check valve. Right: depicting flow paths when the check valve is open

To reduce friction between the rotating valve plate and the fixed tiers, thrust bearings are used. Several thrust bearing types were investigated: rolling-element, hydrodynamic, hydrostatic and magnetic bearings [7] [8].

To determine the thrust bearing type, the axial force on the plate must first be found. This force is a result of the pressure differences:

$$F = \Delta PA = (P_{high} - P_{tank}) \frac{2\pi - \gamma}{2} (R_o^2 - R_i^2) \quad (24)$$

The maximum force on the valve plate was calculated to be approximately 1500 N.

With rolling-element bearings, balls or rollers are used to reduce friction. An advantage of these bearings is that they allow the use of shims for modifying the axial clearance for experimental purposes. However, they result in slightly higher friction than the other bearing types mentioned.

Hydrodynamic and hydrostatic bearings trap lubricant or pressurized fluid between two surfaces. Both bearings have relatively low friction and high damping capacity. However, with hydrodynamic bearings, there is the risk of fluid film lubrication breaking down during starting and stopping; with hydrostatic bearings, an external source is necessary to maintain pressure.

The valve plate can also be “floated” through magnetic levitation. Magnetic bearings are essentially frictionless. They are, however, vulnerable to fluctuating loads, as present in the

on-off valve system. Large magnets are also needed to generate the high load capacity [9]. The implementation of Halbach Arrays into the valve can possibly generate sufficient magnetic force to levitate the valve plate between the two tiers. A particular arrangement of a series of permanent magnets can augment the magnetic field on one side while the field is canceled on the other.

For the purpose of experimentation, mechanical bearings – ball and needle thrust bearings – are used. As mentioned, these permit the use of shims to vary the clearance between the valve plate and the tiers

## CONCLUSIONS

The second generation high-speed on-off valve is currently being manufactured. Experimental testing of the valve will commence shortly.

Future work includes integration of hydrodynamic or magnetic thrust bearings into the valve. An hydraulic accumulator may be integrated into the on-off valve. CFD analysis will also be performed on the valve to find the effects of the complex geometry of the orifices on the valve efficiency. A coupled dynamic analysis with a moving valve plate, or “wall”, will be conducted to find its effects on the fluid flow. Additionally, CFD can aid in the development of the valve, whereby the “weaker” areas of the valve are found and methods to rectify them are implemented and tested virtually.

Work will also be performed on reducing the vibration of the valve plate. Additional goals include decreasing the switching volume and transition times and improving the compactness of the valve. Furthermore, research is being performed on the bulk modulus of the hydraulic fluid and its compressibility.

## REFERENCES

- [1] EPA, 2004, “World's First Full Hydraulic Hybrid SUV”, SAE World Congress.
- [2] Li, P. Y., Li, C. Y., and Chase, T. R., 2005, "Software Enabled Variable Displacement Pumps," ASME International Mechanical Engineering Congress and RD&D Exposition, (81376).
- [3] Katz, A. A. and Van de Ven, J. D., 2009, "Design of a High-Speed On-Off Valve," International Mechanical Engineering Congress & Exposition, (11189).
- [4] Meritt, H., 1967, “Hydraulic Control Systems”, John Wiley & Sons, New York.
- [5] Norton, R. L., 2006, “Machine Design - an Integrated Approach”, Pearson Prentice Hall, New Jersey.
- [6] Cundiff, J. S., 2002, “Fluid Power Circuits and Controls”, CRC Press, New York.
- [7] Hamrock, B. J., Schmid, S. R. and Jacobson, B. O., 1994, “Fundamentals of Fluid Film Lubrication”, Portland : McGraw-Hill, 1994.
- [8] Harnoy, A., 2003, “Bearing Design in Machinery: Engineering Tribology and Lubrication”, Marcel Dekker Inc., New York.
- [9] Ebrahimi, B., Khamesee, M. B. and Golnaraghi, M. F., 2008, “Design and Modeling of a Magnetic Shock Absorber based on Eddy Current Damping Effect”, Journal of Sound and Vibration, **315**(4-5), pp. 875-889.